Published in final edited form as:

Faraday Discuss. ; 241: 266–277. doi:10.1039/d2fd00122e.

Photomechanochemical control over stereoselectivity in the [2+2] photodimerization of acenaphthylene

Sankarsan Biswas[†,a,b,c], **Sayan Banerjee**[†,d], **Milan A. Shlain**[a,b,c], **Andrey A. Bardin**[f,g], **Rein V. Ulijn**[a,b,c,e], **Brent L. Nannenga**[f,g], **Andrew M. Rapped**[d], **Adam B. Braunschweig**[*,a,b,c,e]

[a]Advanced Science Research Center, Graduate Center, City University of New York, 85 St. Nicholas Terrace, New York, NY 10031, USA

[b]Department of Chemistry, Hunter College, 695 Park Avenue, New York, NY 10065, USA

[c]PhD Program in Chemistry, Graduate Center, City University of New York, 365 5th Avenue, New York, NY 10016, USA

[d]Department of Chemistry, University of Pennsylvania, Philadelphia, Pennsylvania 19104–6323, USA

[e]PhD Program in Biochemistry, Graduate Center, City University of New York, 365 5th Avenue, New York, NY 10016, USA

[f]Chemical Engineering, School for Engineering of Matter, Transport, and Energy, Arizona State University, Tempe, AZ 85287, USA.

[g]Center for Applied Structural Discovery, The Biodesign Institute, Arizona State University, Tempe, AZ 85287, USA

Abstract

Tuning solubility and mechanical activation alters the stereoselectivity of the [2+2] photochemical cycloaddition of acenaphthylene. Photomechanochemical conditions produce the *syn* cyclobutane, whereas the solid-state reaction in the absence of mechanical activation provides the *anti*. When the photochemical dimerization occurs in a solubilizing organic solvent, there is no selectivity. Dimerization in H_2O, where acenaphthylene is insoluble, provides the *anti* product. DFT calculations reveal that insoluble and solid-state reactions proceed *via* a covalently bonded excimer, which drives *anti* selectivity. Alternatively, the noncovalently bound *syn* conformer is more mechanosusceptible than the *anti*, meaning it experiences greater destabilization, thereby producing the *syn* product under photomechanochemical conditions. Cyclobutanes are important

[*]Corresponding Author: abraunschweig@gc.cuny.edu. **Corresponding Authors: Adam B. Braunschweig** – Advanced Science Research Center, Graduate Center, City University of New York, 85 St. Nicholas Terrace, New York, NY 10031, USA; **Andrew M. Rappe** – Department of Chemistry, University of Pennsylvania, Philadelphia, Pennsylvania 19104-6323, USA; rappe@sas.upenn.edu.
[†]Contributed equally

Author Contributions

Sankarsan Biswas (S.B.1.) performed the experiments with the guidance from A.B.. Sayan Banerjee (S.B.2.) performed the DFT calculations with the guidance from A.M.R.. S.B.1., S.B.2., A.B., and A.M.R. interpreted the results and wrote the manuscript together. Milan A. Shlain (M.S.A) helped to modify the photoreactor for performing photomechanochemistry. Brent L. Nannenga (B.L.N.) and Andrey Alex Bardin (A. A. B.) performed microED experiments for determining the crystal structure of the photo dimers. Rein V. Ulijn (R.V.U) provided scientific input. All authors have given approval to the final version of the manuscript.

Conflicts of interest

The authors declare no competing financial interests.

components of biologically active natural products and organic materials, and we demonstrate stereoselective methods for obtaining *syn* or *anti* cyclobutanes under mild conditions and without organic solvents. With this work, we validate photomechanochemistry as a viable new direction for the preparation of complex organic scaffolds.

Graphical Abstract

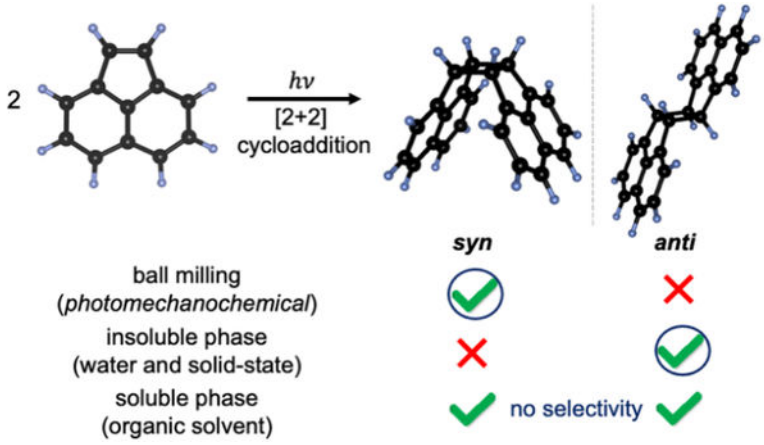

Unique and mutually orthogonal photomechanochemical and photosolvochemical stereoselective routes for cycloaddition of acenaphthylene with high yields have been reported. These methods provide scalable and environmentally benign approaches for stereoselective photocycloaddition reactions.

Keywords

Mechanochemistry; Photochemistry; Cycloaddition; Cyclobutanes; Density Functional Theory

Introduction

Mechanochemistry involves[1–3] the use of force/strain/curvature to make or break chemical bonds, and such methods are attractive because they satisfy all twelve principles of green chemistry.[4] In addition to the minimal environmental impact, the benefits of mechanochemical reactions can include faster reaction kinetics,[5] improved stereoselectivities and yields, or access to stereo- and regioisomers, or other chemical products,[6] that are not accessible by solvothermal methods. Recognizing the advantages of mechanochemistry and the growing suite of tools for performing and studying reactions under force, the diversity of reactions that have been performed mechanochemically is rapidly expanding, and includes the formation of metal-organic frameworks,[7] synthetic polymers,[8] and small molecules.[1, 9] Amongst the reactions that have been most thoroughly studied under mechanochemical activation is the thermally allowed [4+2] Diels-Alder[3, 10, 11] reaction, and it is now known that this reaction can be driven forward with force because of its negative volume of activation.[12–14] The Diels-Alder reaction is an example of a broader class of reactions, the pericyclic cycloadditions,[15] that also have negative activation volumes, and many of these have been carried out mechanochemically as well.[10, 16, 17]

A class of pericyclic reactions which should also possess negative activation volumes, and thus should be accelerated by the application of force, are symmetry-allowed [4n] photochemical cycloadditions, which are widely exploited in organic synthesis to prepare complex molecular scaffolds.[14, 18, 19] The potential benefits of performing photochemical cycloadditions mechanochemically include improved yields and stereochemical control, the latter of which is particularly important as a mixture of stereoisomers are often obtained.[20] Despite these potential advantages, [4n] cycloadditions have not yet been investigated under photomechanochemical conditions – where both illumination and force are applied to the reactants simultaneously – because of challenges associated with developing instrumentation that is capable of illuminating the reactants during compression. To this end, here we implement a new reactor to drive a [2+2] cycloaddition reaction under compression, and, in doing-so, show that such conditions are highly stereoselective as a result of a unique photomechanochemical reaction pathway.

The symmetry-allowed [2+2] photochemical cycloadditions of alkenes to form cyclobutanes,[20] are frequently used to form primary and secondary metabolites[21, 22] with attractive antimicrobial,[23, 24] antibacterial,[24] and analgesic properties,[24] and are increasingly explored as a responsive component of functional materials.[25–27] As a consequence, developing methods for their construction remains a focus of the synthetic community.[23] One challenge that still remains, however, is controlling the stereoselectivity of these photoreactions because an undesired mixture of cyclobutane stereoisomers is often produced.[20, 28–30] For example, the dimerization of acenaphthylene is considered a model reaction for understanding how experimental conditions affect the yields and stereochemical outcomes of [2+2] photocycloadditions.[31–36] In organic solvents, a mixture of *syn* and *anti* isomers of the acenaphthylene dimer is obtained,[37] and, generally, the former is the major product.[34] Strategies to alter the reaction outcome so that the primary product is *anti* include the use of heavy atom solvents,[34] photosensitizers,[34] or a combination of a photosensitizer and a molecular cage,[38] but such conditions often require undesirable solvents, use expensive catalysts, or continue to produce a mixture of isomers. As such, further efforts are needed to understand the drivers of stereoselectivity, which could result in design rules that could be deployed to develop simple, scalable, and widely accessible methods for the stereochemical control of [2+2] photochemical cycloadditions that minimize the use of organic solvents and complex and expensive reagents.

Results and discussion

Here we study the [2+2] photodimerization of acenaphthylene under four different conditions, (i) illumination of the solid-state acenaphthylene under ball milling, (ii) illumination of the solid-state crystal in the absence of ball milling, (iii) illumination in organic solvents (soluble phase), and (iv) illumination in H_2O (insoluble phase). For (i), we find that primarily the *syn* dimer is selectively formed, whereas (ii) and (iv) selectively form the *anti* dimer. Interestingly, we do not observe any noticeable selectivity for (iii). First-principles Density Functional Theory (DFT) calculations reveal that the extent of solubility changes the cycloaddition pathway: for insoluble and solid-state conditions (b and d), the cycloaddition proceeds *via* the formation of a covalently bonded excimer, which is geometrically and energetically closer to the *anti* transition state, thereby explaining the

anti selectivity observed in (ii) and (iv). Additionally, we reveal that the noncovalently bound *syn* dimer is more mechanosusceptible, as it experiences more destabilization upon mechanical compression, which underpins the formation of *syn* product under ball milling (a). Therefore, in addition to providing mild conditions for the selective production of both *syn* and *anti* cyclobutanes that avoid the use of organic solvents, this work lays the foundation for understanding photomechanochemical stereoselectivity, which in turn, could lead to environmentally benign methods for the production of important chemical reagents.

Solid-state [2+2] photocycloaddition of acenaphthylene

We first investigated whether the [2+2] dimerization of acenaphthylene can be driven photomechanochemically and how these conditions affect reaction yield and stereoselectivity. To do so, a ball-mill reactor (SPEXSamplePrep, 8000M) was modified (Figure S1) with a blue LED (HepatoChem, DX Series light 30 W, λ_{max} = 450 nm), and the reaction was run in a glass vial (20 mL) with two methacrylate balls (SPEXSamplePrep, 8006A, 9.5 mm diameter, 350 mg) so that light could reach the reagents during milling. In addition, we found it necessary to fluorinate the vial[39] and add silica gel (SILICYCLE, SilicaFlash® GE60, 70–230 mesh) to the reaction to prevent the reagents from adhering to the side walls. Acenaphthylene (1.2 g) and silica gel (1.2 g) were added to the vial under inert Ar atmosphere, unless otherwise noted, and milled for 20 h at a frequency of 17.7 Hz. Upon completion of the milling, yields and *anti*:*syn* ratios were determined by ^{1}H NMR spectroscopy by dissolving a portion of the crude mixture in $CDCl_3$ followed by filtration to remove silica from the $CDCl_3$ solution. We found (Table 1, entries 1 – 2) that, photomechanochemically, the dimerization reaction proceeded with yields up to 96 % with 6:94 *anti*:*syn* selectivity. Stereochemical assignments were confirmed by ^{1}H NMR spectroscopy and microcrystal electron diffraction[40, 41] on the crystallites isolated from the reactions (Figure S26 and Table S2). This *syn* selectivity and yield were retained in ambient atmosphere. In the absence of the illumination, no product was observed. To put this result in the context, in organic solvents, this reaction favors the *syn* product but with poor selectivity, and high *syn* selectivity has only been obtained using expensive and complex reagents or undesirable organic solvents.[42–45] For example, Kaanumalle *et al.*[46] reported 99 % *syn* product (99 % yield) in borate buffer using an organometallic molecular cage, while Cowan *et al.*[34] obtained 98 % *syn* (39 % yield) selectivity in O_2-saturated benzene. Thus, we find that photomechanochemical conditions provide the mildest route towards the *syn* product of the acenapthylene dimer yet reported.

All reactions were performed at 20 °C. Acenaphthylene samples were irradiated with a blue LED (HepatoChem, DX Series light 30 W, λ_{max} = 450 nm) for 20 h. Yields and selectivities were obtained from ^{1}H NMR in $CDCl_3$. [a] Ball-mill reactions performed in the presence of silica as an additive to prevent the reagents from adhering to the side walls of the reaction vessel. [b] Reactions were performed in a petri dish with ground acenaphthylene crystals and no milling during illumination.

From these experiments it was unclear whether the *syn* selectivity was the result of carrying out the reaction in the solid state or whether force played an active role in dictating stereoselectivity. To determine whether force has a role in stereoselectivity, the reaction

was carried out on acenaphthylene crystals by illuminating them in the absence of force. The acenaphthylene crystals (100 mg) were ground with a mortar and pestle, sealed in a petri dish under either inert or ambient atmosphere, and the crystals were then irradiated with the same blue LED for 20 h (Table 1, entries 3 – 4). Under Ar, we found that the reaction favored the *anti* isomer (70:30 *anti*:*syn*), while ambient atmosphere provided a mixture with a 46:54 *anti*:*syn* ratio. So, in the absence of O_2, more *anti* product forms, but as O_2 is introduced, such selectivity is diminished. This was also observed by Haga *et al.*,[36] who noted that the presence of a triplet quencher (here O_2) reduces the *anti*-selectivity. These results show that the absence of force provides substantially different products than when the products were milled during illumination. Therefore, we find that running the [2+2] photodimerization of acenaphthylene under Ar while milling results in the opposite stereoselectivity than when the reaction is carried out without milling. These observations confirm that a unique photomechanochemical reaction pathway exists for the dimerization of acenaphthylene that is distinct from the pathway followed during irradiation in the absence of force.

[2+2] photocycloaddition of acenaphthylene in solution-state

We then studied the photodimerization of acenaphthylene in different organic solvents with variable H_2O:organic solvent ratios at the room temperature. Here we have examined the photodimerization with 5 different organic solvents that are miscible with H_2O – DMSO, EtOH, MeOH, DMF, and MeCN – along with H_2O itself, under blue light illumination. As acenaphthylene is insoluble in H_2O, these experiments provide insight into the role of solubility on the stereoselectivity. To maximize solvent/acenaphthylene interaction (especially for the solvent mixture where acenaphthylene is poorly soluble), 5 M solution of acenaphthylene was prepared in DMSO, and 4 μL of this stock solution was then added to 1 mL of the desired solvent system to prepare 20 mM solutions of acenaphthylene. The solution was then sonicated for 1 min. The summary of the stereoselectivity observed in these experiments is given in Figure 1C and Table S1. Although, we find that the absolute value of the *anti:syn* ratio varies depending on the nature of the organic solvent, we observe the conspicuous trend that the *anti* selectivity increases with the amount of H_2O, where using just H_2O selectively provides the *anti* product. Because of the insolubility of the acenaphthylene in H_2O, the solution was sonicated to disperse the reactant, which led to a cloudy, opaque solution. Following irradiation, the *anti* isomer was recovered as the major product (84:16 *anti*:*syn*) in 84 % yield. In other words, the insolubility of acenaphthylene favors the *anti* product. This observation is in good agreement with the solid-phase reactions on the crystal in the absence of milling, which also resulted in *anti* stereoselectivity (*anti*:*syn* 70:30). Thus, we conclude that solubility also plays an important role in determining the stereoselectivity. For photocycloadditions, it is known that lowering the reaction temperature can improve regio- and stereoselectivity.[47] As such, the reaction temperature was then lowered to 10 °C, and running the reaction for 16 h in H_2O resulted in quantitative conversion, with *anti*:*syn* reaching 91:9. The *anti* selectivity observed here is similar to those reported by Guo *et al.*[38] who used a molecular cage composed of a Ru^{2+} photocatalyst to achieve 89:11 *anti*:*syn*. So a major challenge in stereocontrolled photochemical cycloadditions – obtaining the *anti* isomer of acenaphthylene as the major

product – was resolved by simply running the reaction in H_2O, which, in addition to providing an otherwise elusive product, is both atom-efficient and environmentally benign.

DFT calculations for the [2+2] photocycloaddition of acenaphthylene in solution-state

We performed DFT calculations[48] to understand why liquid and solid phase reactions result in different stereoisomers. In doing so, we explored the potential energy surfaces by considering the photodimerization pathways from three different initial states– *syn* and *anti* conformers, which are noncovalently bound supramolecular dimers, and a state that consists of two separated monomers (Figure 2). On the other hand, the noncovalently bound *syn* and *anti* conformers correspond to the insoluble solid-state acenaphthylene (and state present in H_2O), when the monomers are close to each other and experience a net stabilizing interaction as compared to separated monomers. We find that the thermal activation barrier for the *anti* product formation (179 kJ/mol) is lower than the *syn* product formation (269 kJ/mol) (Figure 2). Such high barriers suggest that the reactions cannot be performed at room temperature without photoexcitation, which we also observe experimentally. In the soluble-phase scenario, we find that the excited triplet (T) and singlet (S) states of the separated monomers (yellow dotted lines in Figure 2) are above the *syn* and *anti* transition states (TS). Thus, when completely solvated, photoexcitation injects sufficient energy to access both the *anti* and *syn* TS; this in turn, leads to both *syn* and *anti* product formations, explaining the loss of selectivity for this reaction in organic solvents. In the solid state or in H_2O, where the poor solubility keeps the acenaphthylene aggregated, the molecules exist as noncovalently bound *syn* and *anti* supramolecular conformers. We find that the spin-flipped T states for both the *syn* and *anti* supramolecular conformer lead to the formation (shaded cyan region in Figure 2) of a covalently bonded excimer (excimer in Figure 2). Formation of excimers in photochemical reactions have been reported previously[49–51] to have a role in determining the selectivity of the products. Therefore, as the photoexcitation occurs in the insoluble phase, the supramolecular dimers form a covalent bond in the excimer, gaining a stabilization of nearly 117 $kcal \cdot mol^{-1}$ per dimer compared to the vertically excited T state. We find that the geometry of this bonded excimer resembles more closely to the *anti* transition state than the *syn*. Additionally, as the *anti* TS has lower energy than the *syn* TS, energetically it is also easier to access the *anti* TS from the bonded excimer. Thus, the formation of the bonded excimer preferentially leads to the *anti* product. This explains the selective formation of the *anti* product in the insoluble phase, *i.e.* in H_2O and in crystals in the absence of ball milling.

DFT calculations for the [2+2] photocycloaddition of acenaphthylene in solid-state

To understand the origin of *syn* selectivity that occurs under the photomechanochemical conditions, we have applied force (F) along the C–C bond forming vector of the *syn* and *anti* conformations using the external force explicitly induced (EFEI) method.[52, 53] In this simulation, the intertwined effect of F and photoexcitation is not incorporated, rather only the effect of compressive F on stability is studied. We envisage that ball milling exerts compression by bringing the monomers in the *syn* and the *anti* supramolecular conformers closer to each other. Thus, applying forces along the C–C bonds in the simulation (as shown in Figure 3A) can have an effect similar to what occurs in a ball mill. We find that the *syn* conformer undergoes bond formation at lower F (between 8 nN and 9 nN),

compared to the *anti* dimer (between 12 nN and 13 nN), which is shown by the grey shaded regions in Figure 3B. To understand why the *syn* supramolecular conformer is more susceptible to *F*, we examined the *F* range of 5–8 nN with more datapoints. The reaction coordinate (*RC*) in Figure 3C is defined based on the C–C distance, wherein the bond distances at 5 nN and 8.55 nN correspond to *RC* of 0 and 1, respectively. We find that the slope of *RC vs. F* (black dashed lines in Figure 3C) is higher for the *syn* supramolecular conformer. This shows that a more significant change in *RC* is attained for *syn* than *anti* at the same applied *F*. In other words, the results directly confirm that *syn* supramolecular conformer is more mechanosusceptible, meaning that its *RC* has a stronger dependence on *F*. In addition, the *syn* supramolecular conformer experiences more destabilization for the same applied *F* than the *anti* (filled markers in Figure 3C). To analyze these effects, we implement the energy decomposition analysis (EDA)[54] to understand the origin of the mechanosusceptibility by quantifying the interaction energy between the acenaphthylene monomers (Figure 3D). EDA consists of three terms: frozen density (E_{FZ}), charge transfer (E_{CT}), and polarization (E_{Pol}).[54] We find that the E_{FZ} dominates in the higher *F* regime, and it increases drastically near 7–8.55 nN for the *syn*, but *anti* does not exhibit such behavior (Figure 3D). As E_{FZ} captures the interaction between the unrelaxed electron density between the monomers, we conclude that the face-to-face orientation of the π-clouds of the *syn* supramolecular conformer, and the resulting repulsion at smaller distances, make it more mechanosusceptible, whereas for the *anti* supramolecular dimer, π-clouds interact to a lesser extent. Additionally, it is worth noting that the TS for the *syn* product formation corresponds solely to compression along the C–C bonds participating in the [2+2] cycloaddition (*syn* TS in Figure 2). On the other hand, for the *anti* product formation, shear force also plays an important role along with compression as the monomers need to slide to form the *anti* product (*anti* TS in Figure 2). We conjecture that as attaining shear and compression simultaneously is statistically less probable under ball milling than just compression, *syn* selectivity is boosted. Thus, these results explain qualitatively the stereoselectivity of solid-state photomechanochemical conditions.

Conclusion

In conclusion, we have studied the [2+2] dimerization of acenaphthylene and explored how light, force, and solvent can be combined to achieve both *syn* and *anti* stereoselective photodimerization. We find that *syn* stereoselectivity is observed under photomechanochemical conditions because of the greater mechanosusceptibility of the noncovalently bound *syn* supramolecular conformer compared to the *anti* conformer. In studying how solvents and solubility affect yields and stereoselectivity, we have shown that simply running the photodimerization in H_2O provides the *anti* dimer in high yields, and these conditions provide among the highest anti stereoselectivity yet observed because of the formation of a bonded excimer in insoluble phases. Thus, we report scalable and mild conditions for obtaining both *syn* and *anti* [2+2] cycloaddition products without necessitating organic solvent or complex additional reagents. More importantly, we demonstrate that photomechanochemical pathways exist that are distinct from solvothermal or solid-state reaction pathways, and we explain stereochemistry based upon mechanosusceptibility, a concept that may be used to predict stereoselectivity for other

mechanochemical reactions as well. In doing so, have shown that photomechanochemistry and photosolvochemistry can provide mutually orthogonal stereoselective routes for making complex organic scaffolds. Therefore, photomechanochemistry merits further investigation as a scalable and environmentally benign approach to stereoselective photochemistry.

Experimental Section

Experimental procedures, synthesis, and characterization of all new compounds, NMRs, Microcrystalline electron diffraction are provided in the supporting information file.

Supplementary Material

Refer to Web version on PubMed Central for supplementary material.

Acknowledgement

A.B.B. and A.M. R. acknowledge support from the National Science Foundation Center for Mechanical Control of Chemistry (CHE-2023644). The NMR data (Bruker Avance 300 MHz) presented herein were collected in part at the CUNY ASRC Biomolecular NMR facility and the NMR facility of the City College of the CUNY. Mass spectra were collected at the CUNY ASRC Biomolecular Mass Spectrometry Facility. S.B.2. acknowledges a graduate fellowship from the Vagelos Institute of Energy Science and Technology. B.L.N. acknowledges support from the National Institutes of Health grant number R21GM135784, and the use of the Titan Krios within the Eyring Materials Center at Arizona State University (NSF DBI 1531991).

References

1. O'Neill RT and Boulatov R, Nat. Rev. Chem, 2021, 5, 148–167.
2. Do J-L and Friščić T, ACS Cent. Sci, 2017, 3, 13–19. [PubMed: 28149948]
3. Hernández JG and Bolm C, J. Org. Chem, 2017, 82, 4007–4019. [PubMed: 28080050]
4. Mateti S, Mathesh M, Liu Z, Tao T, Ramireddy T, Glushenkov AM, Yang W and Chen YI, Chem. Commun, 2021, 57, 1080–1092.
5. Qi Y, Yang J and Rappe AM, ACS Appl. Mater. Interfaces, 2016, 8, 7529–7535. [PubMed: 26910803]
6. Yang F, Yang J, Qi Y, de Boer MP, Carpick RW, Rappe AM and Srolovitz DJ, ACS Appl. Mater. Interfaces, 2019, 11, 39238–39247. [PubMed: 31547645]
7. Chen D, Zhao J, Zhang P and Dai S, Polyhedron, 2019, 162, 59–64.
8. Chen Y, Mellot G, van Luijk D, Creton C and Sijbesma RP, Chem. Soc. Rev, 2021, 50, 4100–4140. [PubMed: 33543174]
9. Achar TK, Bose A and Mal P, Beilstein J. Org. Chem, 2017, 13, 1907–1931. [PubMed: 29062410]
10. Han X, Bian S, Liang Y, Houk KN and Braunschweig AB, J. Am. Chem. Soc, 2014, 136, 10553–10556. [PubMed: 25028773]
11. Bian S, Scott AM, Cao Y, Liang Y, Osuna S, Houk KN and Braunschweig AB, Journal of the American Chemical Society, 2013, 135, 9240–9243. [PubMed: 23758146]
12. Breslow R, Acc. Chem. Res, 1991, 24, 159–164.
13. Meijer A, Otto S and Engberts JBFN, J. Org. Chem, 1998, 63, 8989–8994.
14. Chen B, Hoffmann R and Cammi R, Angewandte Chemie International Edition, 2017, 56, 11126–11142. [PubMed: 28738450]
15. Herndon WC, Chem. Rev, 1972, 72, 157–179.
16. Mehlich J and Ravoo BJ, Org. Biomol. Chem, 2011, 9, 4108–4115. [PubMed: 21494705]
17. Rozkiewicz DI, Jańczewski D, Verboom W, Ravoo BJ and Reinhoudt DN, Angew. Chem. Int. Ed, 2006, 45, 5292–5296.
18. CRC Handbook of Organic Photochemistry and Photobiology, CRC Press, Boca Raton, 2012.

19. Klärner F-G and Diedrich MK, in The Chemistry of Dienes and Polyenes, 1997, pp. 547–617.
20. Poplata S, Tröster A, Zou Y-Q and Bach T, Chem. Rev, 2016, 116, 9748–9815. [PubMed: 27018601]
21. Sergeiko A, Poroikov VV, Hanus LO and Dembitsky VM, Open Med Chem J, 2008, 2, 26–37. [PubMed: 19696873]
22. Dembitsky VM, Journal of Natural Medicines, 2008, 62, 1–33. [PubMed: 18404338]
23. Li J, Gao K, Bian M and Ding H, Organic Chemistry Frontiers, 2020, 7, 136–154.
24. Sergeiko A, Poroikov VV, Hanus LO and Dembitsky VM, Open Med Chem J, 2008, 2, 26–37. [PubMed: 19696873]
25. Yang J, Horst M, Romaniuk JAH, Jin Z, Cegelski L and Xia Y, J. Am. Chem. Soc, 2019, 141, 6479–6483. [PubMed: 30969109]
26. Chen Z, Mercer JAM, Zhu X, Romaniuk JAH, Pfattner R, Cegelski L, Martinez TJ, Burns NZ and Xia Y, Science, 2017, 357, 475–479. [PubMed: 28774923]
27. Chen Z, Zhu X, Yang J, Mercer JAM, Burns NZ, Martinez TJ and Xia Y, Nat. Chem, 2020, 12, 302–309. [PubMed: 31907403]
28. Ramamurthy V and Mondal B, J. Photochem. Photobiol. C: Photochem. Rev, 2015, 23, 68–102.
29. Yoon TP, Acc. Chem. Res, 2016, 49, 2307–2315. [PubMed: 27505691]
30. Wang J-S, Wu K, Yin C, Li K, Huang Y, Ruan J, Feng X, Hu P and Su C-Y, Nat. Commun, 2020, 11, 4675. [PubMed: 32938933]
31. Samanta A, Devadoss C and Fessenden RW, J Phys Chem, 1990, 94, 7106–7110.
32. Bowen EJ and Marsh JDF, J. Am. Chem. Soc, 1947, DOI: 10.1039/JR9470000109, 109–110.
33. Livingston R and Wei KS, J Phys Chem, 1967, 71, 541–547.
34. Cowan DO and Drisko RLE, J. Am. Chem. Soc, 1970, 92, 6286–6291.
35. White EH, Wildes PD, Wiecko J, Doshan H and Wei CC, J. Am. Chem. Soc, 1973, 95, 7050–7058.
36. Haga N, Takayanagi H and Tokumaru K, J. Org. Chem, 1997, 62, 3734–3743.
37. Dziewoński K and Rapalski G, Ber. Dtsch. Chem. Ges, 1912, 45, 2491–2495.
38. Guo J, Fan Y-Z, Lu Y-L, Zheng S-P and Su C-Y, Angew. Chem. Int. Ed, 2020, 59, 8661–8669.
39. Eichelsdoerfer DJ, Liao X, Cabezas MD, Morris W, Radha B, Brown KA, Giam LR, Braunschweig AB and Mirkin CA, Nat. Protoc, 2013, 8, 2548–2560. [PubMed: 24263094]
40. Levine AM, Bu G, Biswas S, Tsai EHR, Braunschweig AB and Nannenga BL, Chem. Commun, 2020, 56, 4204–4207.
41. Nannenga BL and Gonen T, Nat Methods, 2019, 16, 369–379. [PubMed: 31040436]
42. Karthikeyan S and Ramamurthy V, Tetrahedron Lett, 2005, 46, 4495–4498.
43. Yoshizawa M, Takeyama Y, Okano T and Fujita M, J. Am. Chem. Soc, 2003, 125, 3243–3247. [PubMed: 12630879]
44. Takaoka K, Kawano M, Ozeki T and Fujita M, Chem. Commun, 2006, DOI: 10.1039/B600812G, 1625–1627.
45. Yoshizawa M, Takeyama Y, Kusukawa T and Fujita M, Angew. Chem. Int. Ed, 2002, 41, 1347–1349.
46. Kaanumalle LS and Ramamurthy V, Chem. Commun, 2007, DOI: 10.1039/B615937K, 1062–1064.
47. Yabuno Y, Hiraga Y, Takagi R and Abe M, J. Am. Chem. Soc, 2011, 133, 2592–2604. [PubMed: 21306157]
48. Shao Y, Molnar LF, Jung Y, Kussmann J, Ochsenfeld C, Brown ST, Gilbert ATB, Slipchenko LV, Levchenko SV, O'Neill DP, DiStasio RA Jr, Lochan RC, Wang T, Beran GJO, Besley NA, Herbert JM, Yeh Lin C, Van Voorhis T, Hung Chien S, Sodt A, Steele RP, Rassolov VA, Maslen PE, Korambath PP, Adamson RD, Austin B, Baker J, Byrd EFC, Dachsel H, Doerksen RJ, Dreuw A, Dunietz BD, Dutoi AD, Furlani TR, Gwaltney SR, Heyden A, Hirata S, Hsu C-P, Kedziora G, Khalliulin RZ, Klunzinger P, Lee AM, Lee MS, Liang W, Lotan I, Nair N, Peters B, Proynov EI, Pieniazek PA, Min Rhee Y, Ritchie J, Rosta E, David Sherrill C, Simmonett AC, Subotnik JE, Lee Woodcock Iii H, Zhang W, Bell AT, Chakraborty AK, Chipman DM, Keil FJ, Warshel A, Hehre WJ, Schaefer Iii HF, Kong J, Krylov AI, Gill PMW and Head-Gordon M, Phys. Chem. Chem. Phys, 2006, 8, 3172–3191. [PubMed: 16902710]

49. Wang Y, Haze O, Dinnocenzo JP, Farid S, Farid RS and Gould IR, J. Org. Chem, 2007, 72, 6970–6981. [PubMed: 17676917]
50. Mattay J, Angew. Chem. Int. Ed, 2007, 46, 663–665.
51. Wilzbach KE and Kaplan L, J. Am. Chem. Soc, 1971, 93, 2073–2074.
52. Ribas-Arino J and Marx D, Chem. Rev, 2012, 112, 5412–5487. [PubMed: 22909336]
53. Ribas-Arino J, Shiga M and Marx D, Angew. Chem. Int. Ed, 2009, 48, 4190–4193.
54. Khaliullin RZ, Cobar EA, Lochan RC, Bell AT and Head-Gordon M, J. Phys. Chem. A, 2007, 111, 8753–8765. [PubMed: 17655284]

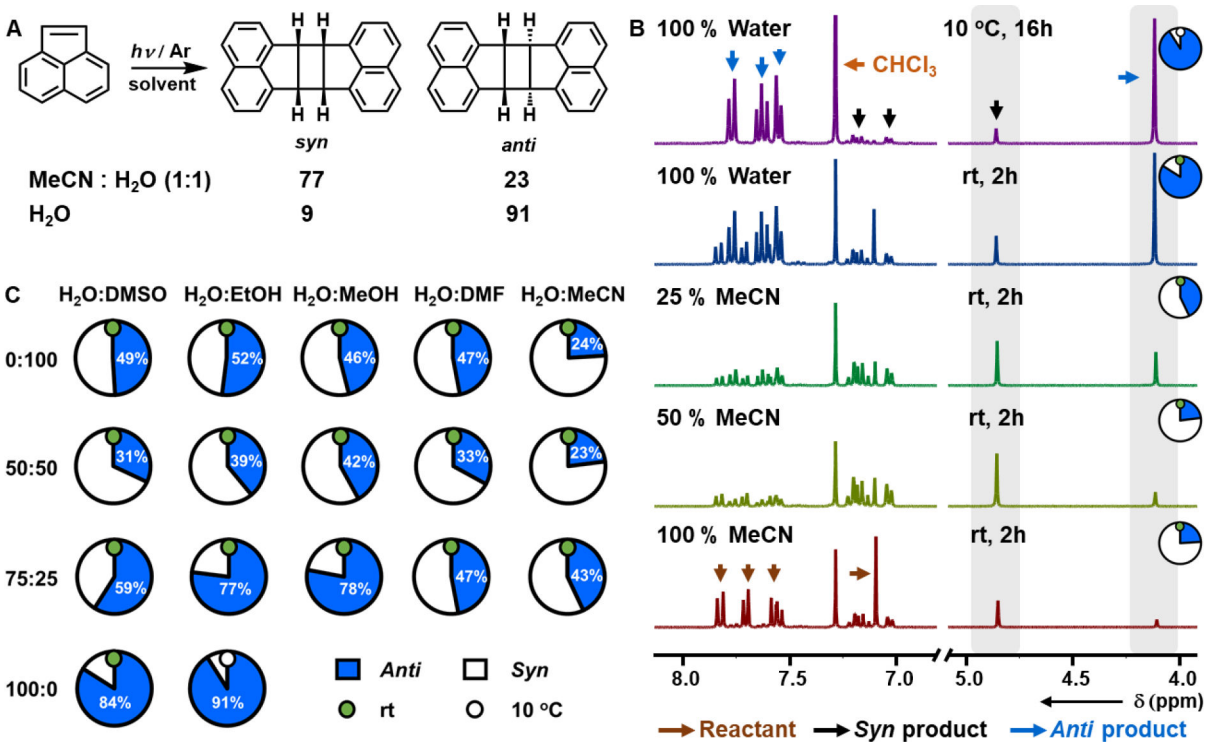

Figure 1.

(A) [2+2] Photocycloaddition of acenaphthylene, with the most stereoselective conditions for syn and anti dimers noted. (B) ^{1}H NMR (300 MHz, $CDCl_3$) of the products of the [2+2] photocycloaddition of acenaphthylene in a binary solvent mixture composed of different ratios of MeCN and H_2O. (C) Change in selectivity with changing solvent composition for the [2+2] photocycloaddition of acenaphthylene in binary solvent mixtures.

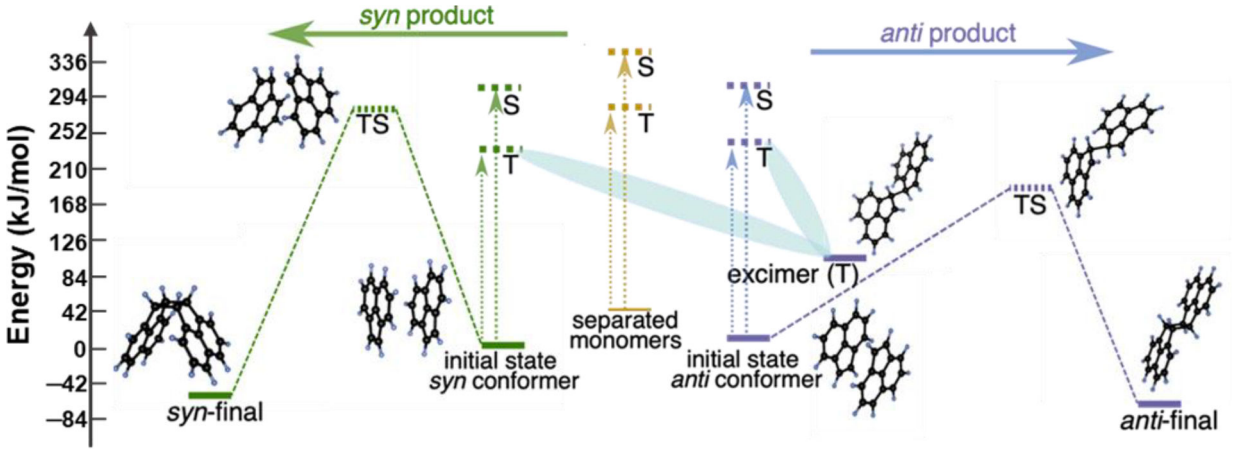

Figure 2.

Potential energy surface obtained using the geometries at the B3LYP-D3/6-31G(d) level of theory showing the pathways for *syn* and *anti* product formation. The abbreviations are as follows: T: Triplet; S: Singlet; TS: Transition state. Dotted arrows represent vertical photoexcitation, and cyan shading illustrates relaxation of the triplet conformer states to the excimer.

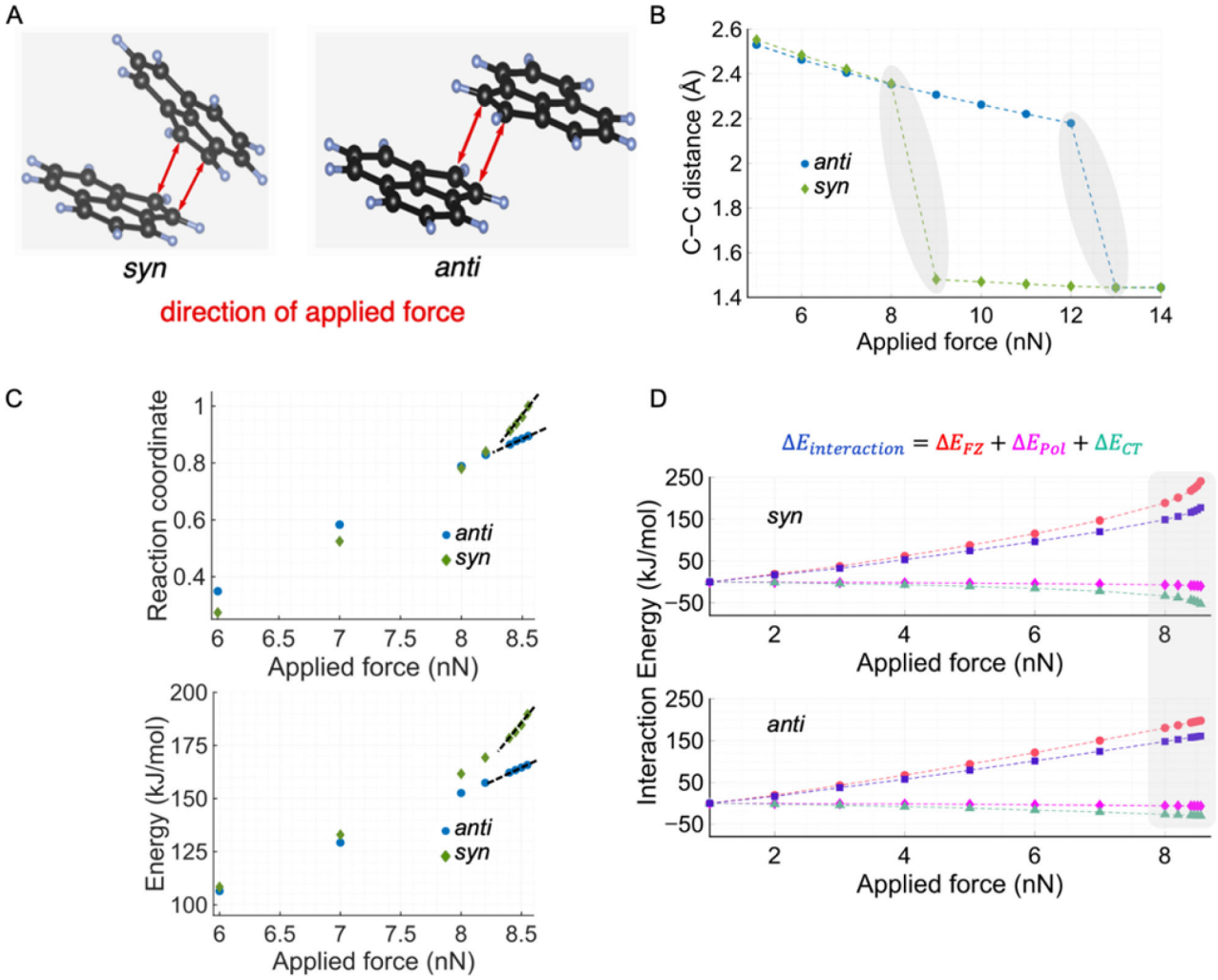

Figure 3.

Effect of force on the dimerization of *syn* and *anti* supramolecular conformers. (A) The directions of the applied forces in simulations using the external force explicitly included (EFEI) method are shown. (B) The effect of applied force on C–C bond formation for *syn* and *anti* conformers. The shaded regions indicate where the *syn* and/or *anti* dimers undergo covalent C–C bond formation from a noncovalent conformer. (C) The change in reaction coordinate (*RC*) and energy (*E*) as a function of the applied force. The *RC* is defined based on the C–C distance, wherein distances at 5 nN and 8.55 nN correspond to *RC* 0 and 1, respectively. The filled circles/diamonds correspond to the *E* values, whereas unfilled markers indicate the change in the *RC*. (D) Energy decomposition analysis showing the effect of force on different inter-action terms between the monomers. The abbreviations are: FZ: frozen density, CT: charge transfer, Pol: polarization.

Table 1.

Solid-state [2+2] photocycloaddition of acenaphthylene.

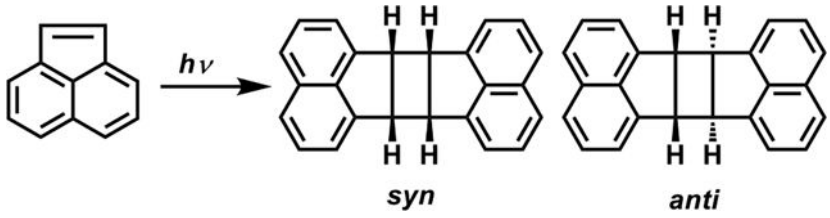

Entry	Atm.	Total Product Yield (%)	*Anti* : *Syn*
1 [a]	Ar	95	6:94
2 [a]	air	87	8:92
3 [b]	Ar	65	70:30
4 [b]	air	99	46:54

All reactions were performed at 20 °C. Acenaphthylene samples were irradiated with a blue LED (HepatoChem, DX Series light 30 W, λ_{max} = 450 nm) for 20 h. Yields and selectivities were obtained from ^{1}H NMR in $CDCl_3$.

*[a]*Ball-mill reactions performed in the presence of silica as an additive to prevent the reagents from adhering to the side walls of the reaction vessel.

*[b]*Reactions were performed in a petri dish with ground acenaphthylene crystals and no milling during illumination.